

Kaon semileptonic form factors at the physical quark masses on large volumes in $N_f = 2 + 1$ lattice QCD

Takeshi Yamazaki^{a,b}, Ken-ichi Ishikawa^{c,d}, Naruhito Ishizuka^b,
 Yoshinobu Kuramashi^b, Yusuke Namekawa^e, Yusuke Taniguchi^b,
 Naoya Ukita^b, and Tomoteru Yoshié^b

(PACS Collaboration)

^aFaculty of Pure and Applied Sciences, University of Tsukuba, Tsukuba, Ibaraki 305-8571, Japan

^bCenter for Computational Sciences, University of Tsukuba, Tsukuba, Ibaraki 305-8577, Japan

^cGraduate School of Advanced Science and Engineering, Hiroshima University, Higashi-Hiroshima, Hiroshima 739-8526, Japan

^dCore of Research for the Energetic Universe, Graduate School of Advanced Science and Engineering, Hiroshima University, Higashi-Hiroshima, Hiroshima 739-8526, Japan

^eEducation and Research Center for Artificial Intelligence and Data Innovation, Hiroshima University, Hiroshima 730-0053, Japan

E-mail: yamazaki@het.ph.tsukuba.ac.jp

Abstract. We present our results for the kaon semileptonic form factors calculated by using two sets of the PACS10 configuration, whose physical volumes are more than $(10 \text{ fm})^4$ at the physical light and strange quark masses in the $N_f = 2 + 1$ lattice QCD. The configurations were generated using the Iwasaki gauge action and $N_f = 2 + 1$ stout-smeared clover quark action. The form factors near zero momentum transfer q^2 can be calculated thanks to the large volume. Using our data, a q^2 interpolation and continuum extrapolation are carried out simultaneously. The value of $|V_{us}|$ is determined using the result of the form factors at $q^2 = 0$ in the continuum limit. Our result of $|V_{us}|$ is compared with the one determined from the CKM matrix unitarity and with those determined using recent lattice results.

1. Introduction

One of the CKM matrix elements $|V_{us}|$ might be a candidate of a signal beyond the standard model (BSM). The value of $|V_{us}|$ determined using the most accurate kaon semileptonic ($K_{\ell 3}$) form factor [1] at zero momentum transfer $q^2 = 0$ is 3 to 5 σ away from those obtained through the CKM matrix unitarity using $|V_{ud}|$ [2, 3]. Furthermore, the value of the $K_{\ell 3}$ determination is slightly different from that of the kaon leptonic ($K_{\ell 2}$) determination [4]. To confirm the discrepancies, it is important to calculate the $K_{\ell 3}$ form factor by different groups. For this purpose, we calculate the $K_{\ell 3}$ form factor using the PACS10 configurations [5, 6]. They were generated on huge volumes of more than $(10 \text{ fm})^3$ at the physical quark masses in $N_f = 2 + 1$ lattice QCD. It is possible to remove major systematic errors in the lattice QCD, *i.e.*, the chiral extrapolation and finite volume effect, by using the PACS10 configurations. We will present our progress in the calculation for the $K_{\ell 3}$ form factors.

All the results in this report were already presented in our recent paper [7].



Content from this work may be used under the terms of the [Creative Commons Attribution 3.0 licence](https://creativecommons.org/licenses/by/3.0/). Any further distribution of this work must maintain attribution to the author(s) and the title of the work, journal citation and DOI.

Table 1. Simulation parameters. The lattice spacing (a), spatial and temporal extents (L, T), and the π and K meson masses (M_π, M_K) are summarized.

a [fm]	$L^3 \times T$	L [fm]	M_π [MeV]	M_K [MeV]
0.063	160^4	10.2	137	501
0.085	128^4	10.9	135	497

2. Results

The 3-point function calculations for the $K_{\ell 3}$ form factors are performed on the two ensembles of the PACS10 configurations, whose spatial extent is more than 10 fm at the physical quark masses. We employ the Iwasaki gauge action and $N_f = 2 + 1$ stout-smeared clover quark action in the configuration generation. Details of the configuration generations are explained in Refs. [5, 6]. The same quark action is used in the calculation of the 3-point functions. The simulation parameters are tabulated in Table 1.

The $K_{\ell 3}$ form factor $f_+(q^2)$ is defined by the matrix elements,

$$\langle \pi(\vec{p}_\pi) | V_\mu | K(\vec{p}_K) \rangle = (p_K + p_\pi)_\mu f_+(q^2) + (p_K - p_\pi)_\mu f_-(q^2), \quad (1)$$

where $q^2 = -(M_K - E_\pi)^2 + \vec{p}_\pi^2$ is the momentum transfer squared. The scalar form factor $f_0(q^2)$ is defined by $f_+(q^2)$ and $f_-(q^2)$ as,

$$f_0(q^2) = f_+(q^2) + \frac{-q^2}{M_K^2 - M_\pi^2} f_-(q^2). \quad (2)$$

The two form factors are extracted from the 3-point functions with the vector current V_μ . We employ two types of the vector current: the local current and point splitting conserved current. For the renormalization of the local vector current, we employ the renormalization factor $Z_V = 1/\sqrt{F_\pi^{\text{bare}}(0)F_K^{\text{bare}}(0)}$, where $F_\pi^{\text{bare}}(0)$ and $F_K^{\text{bare}}(0)$ are the unrenormalized electromagnetic form factors for π and K at $q^2 = 0$ with the local vector current. The two currents give different form factors at a finite lattice spacing, while they should coincide in the continuum limit. Using the two current data at the two lattice spacings, we will discuss the continuum extrapolation of the form factor.

Figure 1 presents the results for $f_+(q^2)$ and $f_0(q^2)$ in a function of q^2 with the local current. Thanks to the large volume, we can calculate the form factors in the $q^2 = 0$ region at both the lattice spacings. The data of $f_+(q^2)$ at the two lattice spacings seem to be explained by a smooth function of q^2 . It means that the finite lattice spacing effects are small in $f_+(q^2)$ using the local vector current. Similar to $f_+(q^2)$, the data of $f_0(q^2)$ with the two lattice spacing near $q^2 = 0$ have a small finite lattice spacing effect, although there is a visible discrepancy in the smaller q^2 region. In contrast to the local current data, the conserved current data have larger finite lattice spacing effects [7].

A q^2 interpolation and continuum extrapolation for the form factors are carried out simultaneously using the two current data at the two lattice spacings. The fit forms are based on the formulas in the next-to-leading order (NLO) SU(3) chiral perturbation theory (ChPT) [8, 9] with additional terms for finite lattice spacing effects. We choose three types of the polynomial function to investigate stability of the fit result. The constraint of $f_+(0) = f_0(0)$ is included in the fit forms. The explicit forms of the fit functions are shown in Ref. [7].

The continuum extrapolation of $f_+(0)$ is presented in the left panel of Fig. 2. The data at each lattice spacing are estimated from a q^2 interpolation with the fit forms based on the NLO

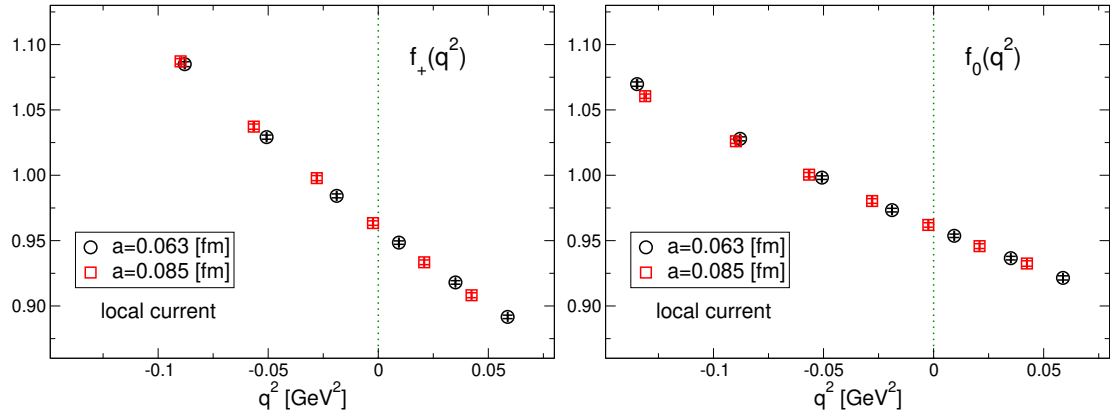


Figure 1. $K_{\ell 3}$ form factors, $f_+(q^2)$ and $f_0(q^2)$, in a function of q^2 using the local vector current. The different symbols express different lattice spacings.

SU(3) ChPT formula using the local and conserved current data separately. The local current data have a flat behavior against the lattice spacing, which can be expected from Fig. 1. In contrast to the local current data, the conserved ones have a clear a dependence. From the observations, we empirically adopt a constant and linear fit forms for the local and conserved current data, respectively, in a continuum extrapolation. In this fit, we assume that the two data agree with each other in the continuum limit. The fit result is denoted by “fit A” in the figure. To investigate the stability of the continuum extrapolation, we also employ quadratic fit forms for both the data. The result represented by “fit B” in the figure has a larger value than the one of fit A.

The right panel of Fig. 2 presents a comparison of the results of $f_+(0)$ obtained from various analyses, such as using different q^2 fit forms and different data sets. The upper two results, fit A and B, correspond to the ones in the left panel of Fig. 2. The fit C result is obtained from a similar fit form to fit A in a continuum extrapolation. Apart from the upper three results, the analyses are carried out using different fit forms for q^2 interpolations and different data sets with the same fit form as fit A for a continuum extrapolation. All the analyses are in good agreement, except for the fit B result. A systematic error in the result is estimated from this discrepancy. It should be noted that if we use the fit B form for continuum extrapolations in the analyses using different fit forms for q^2 interpolations and different data sets instead of the fit A form, similar results are obtained to the fit B result in the figure. This is because we include the fit B result in the systematic error estimate. The fit form dependence in the continuum extrapolation is expected to be largely reduced, if data at a smaller lattice spacing is added in a continuum extrapolation. It is an important future work in our calculation, and we are generating the third PACS10 configuration at a smaller lattice spacing.

Our result of $f_+(0)$ is plotted in the left panel of Fig. 3 together with previous calculations [10, 11, 12, 13, 14, 15, 16, 17, 18, 1, 19]. Our result is roughly consistent with those results within 2σ in the total error. Combining the result of $f_+(0)$ and $|V_{us}|f_+(0) = 0.21654(41)$ [20], the value of $|V_{us}|$ is determined. Our result is shown in the right panel of Fig. 3. Some recent results determined using the $K_{\ell 3}$ form factor [14, 15, 16, 18, 1, 19] are also plotted together with the ones from the $K_{\ell 2}$ decay process [4, 7] and from $|V_{ud}|$ [2, 3] through the unitarity of the CKM matrix. Our result agrees with the ones of the $K_{\ell 2}$ determination. On the other hand, it deviates from the recent $K_{\ell 3}$ determinations and the CKM unitarity with $|V_{ud}|$, while the differences are not so significant, which is less than 3σ . For the BSM physics search, it is important to reduce our large systematic error. To do this, we plan to calculate the $K_{\ell 3}$ form factor at a smaller

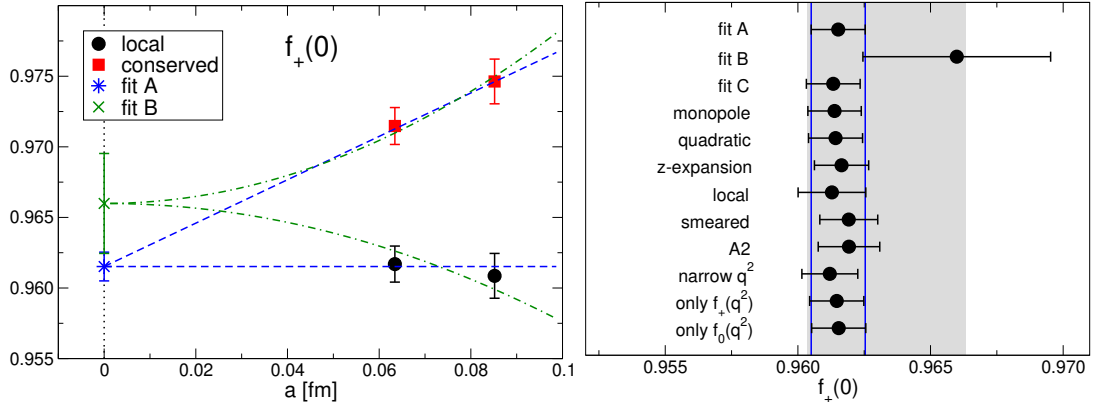


Figure 2. Left: Continuum extrapolation of $f_+(0)$ with the local and conserved current data. The horizontal axis is the lattice spacing. The dashed line and dot-dashed curve represent fit results with different polynomial functions for the continuum extrapolation. **Right:** Comparison of the fit results of $f_+(0)$ in the continuum limit with various analyses. The upper three results are analyzed with different functions of the continuum extrapolation. Other results are obtained from analyses with different fit forms in q^2 interpolations and different data sets. The solid lines and gray band express the statistical and the total errors, respectively. The total error is evaluated from the statistical and systematic errors added in quadrature.

lattice spacing.

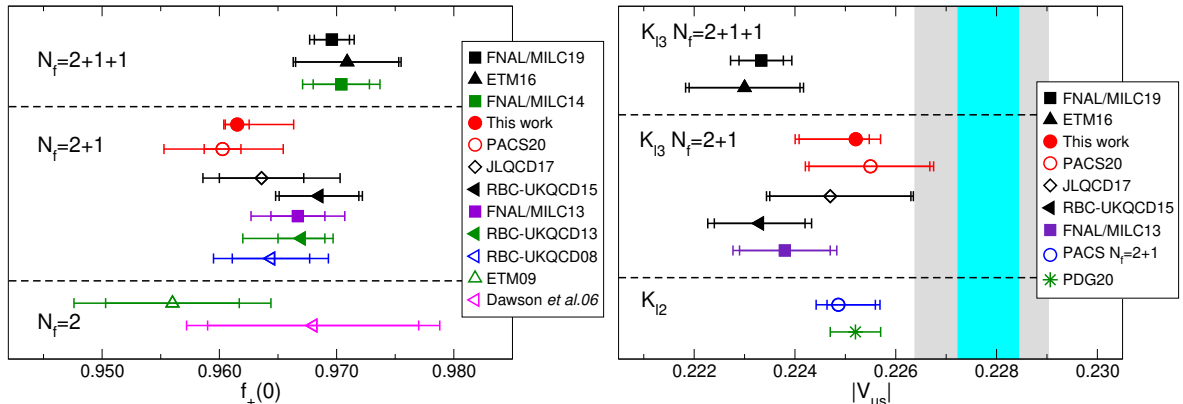


Figure 3. Left: Comparison of our result of $f_+(0)$ with those calculated in previous works [10, 11, 12, 13, 14, 15, 16, 17, 18, 1, 19]. The inner and outer errors express the statistical and total errors. The total error is evaluated from the statistical and systematic errors added in quadrature. **Right:** Comparison of our value of $|V_{us}|$ with those for previous calculations [14, 15, 16, 18, 1, 19] together with the ones determined from the $K_{\ell 2}$ decay process [4, 7]. The light blue and gray bands represent $|V_{us}|$ determined from the unitarity of the CKM matrix using $|V_{ud}|$ in Refs. [2] and [3], respectively.

3. Summary

We have calculated the $K_{\ell 3}$ form factors using the two ensembles of the PACS10 configurations, whose spatial extent is more than 10 fm at the physical quark masses. The result of $f_+(0)$ in the

continuum limit has a large systematic error, which is mainly caused by the fit-form dependence in the continuum extrapolation. Using our result of $f_+(0)$, the value of $|V_{us}|$ is determined. It is consistent with the ones from the $K_{\ell 2}$ determination, and roughly agrees with the ones from the recent $K_{\ell 3}$ determination and the unitarity of the CKM matrix with $|V_{ud}|$. An important future work is a reduction of the systematic error arising from the continuum extrapolation. For this purpose, we plan to repeat the calculation at a smaller lattice spacing.

Acknowledgments

Numerical calculations in this work were performed on Oakforest-PACS in Joint Center for Advanced High Performance Computing (JCAHPC) under Multidisciplinary Cooperative Research Program of Center for Computational Sciences, University of Tsukuba. This research also used computational resources of Oakforest-PACS by Information Technology Center of the University of Tokyo, and of Fugaku by RIKEN CCS through the HPCI System Research Project (Project ID: hp170022, hp180051, hp180072, hp180126, hp190025, hp190081, hp200062, hp200167, hp210112, hp220079). The calculation employed OpenQCD system¹. This work was supported in part by Grants-in-Aid for Scientific Research from the Ministry of Education, Culture, Sports, Science and Technology (Nos. 18K03638, 19H01892). This work was supported by the JLDG constructed over the SINET5 of NII.

References

- [1] Bazavov A *et al.* (Fermilab Lattice, MILC) 2019 *Phys. Rev.* **D99** 114509 (*Preprint* 1809.02827)
- [2] Seng C Y, Gorchtein M, Patel H H and Ramsey-Musolf M J 2018 *Phys. Rev. Lett.* **121** 241804 (*Preprint* 1807.10197)
- [3] Hardy J C and Towner I S 2020 *Phys. Rev. C* **102** 045501
- [4] Zyla P A *et al.* (Particle Data Group) 2020 *PTEP* **2020** 083C01
- [5] Ishikawa K I, Ishizuka N, Kuramashi Y, Nakamura Y, Namekawa Y, Taniguchi Y, Ukita N, Yamazaki T and Yoshié T (PACS) 2019 *Phys. Rev.* **D99** 014504 (*Preprint* 1807.06237)
- [6] Shintani E and Kuramashi Y (PACS) 2019 *Phys. Rev. D* **100** 034517 (*Preprint* 1902.00885)
- [7] Ishikawa K I, Ishizuka N, Kuramashi Y, Namekawa Y, Taniguchi Y, Ukita N, Yamazaki T and Yoshié T (PACS) 2022 *Phys. Rev. D* **106** 094501 (*Preprint* 2206.08654)
- [8] Gasser J and Leutwyler H 1985 *Nucl. Phys.* **B250** 517–538
- [9] Gasser J and Leutwyler H 1985 *Nucl. Phys.* **B250** 465–516
- [10] Dawson C, Izubuchi T, Kaneko T, Sasaki S and Soni A 2006 *Phys. Rev.* **D74** 114502 (*Preprint* hep-ph/0607162)
- [11] Lubicz V, Mescia F, Simula S and Tarantino C (ETM) 2009 *Phys. Rev.* **D80** 111502 (*Preprint* 0906.4728)
- [12] Bazavov A *et al.* (Fermilab Lattice, MILC) 2013 *Phys. Rev.* **D87** 073012 (*Preprint* 1212.4993)
- [13] Boyle P A, Juttner A, Kenway R D, Sachrajda C T, Sasaki S, Soni A, Tweedie R J and Zanotti J M (RBC-UKQCD) 2008 *Phys. Rev. Lett.* **100** 141601 (*Preprint* 0710.5136)
- [14] Boyle P A, Flynn J M, Garron N, Jüttner A, Sachrajda C T, Sivalingam K and Zanotti J M (RBC-UKQCD) 2013 *JHEP* **08** 132 (*Preprint* 1305.7217)
- [15] Boyle P A *et al.* (RBC-UKQCD) 2015 *JHEP* **06** 164 (*Preprint* 1504.01692)
- [16] Aoki S, Cossu G, Feng X, Fukaya H, Hashimoto S, Kaneko T, Noaki J and Onogi T (JLQCD) 2017 *Phys. Rev.* **D96** 034501 (*Preprint* 1705.00884)
- [17] Bazavov A *et al.* (Fermilab Lattice, MILC) 2014 *Phys. Rev. Lett.* **112** 112001 (*Preprint* 1312.1228)
- [18] Carrasco N, Lami P, Lubicz V, Riggio L, Simula S and Tarantino C (ETM) 2016 *Phys. Rev.* **D93** 114512 (*Preprint* 1602.04113)
- [19] Kakazu J, Ishikawa K I, Ishizuka N, Kuramashi Y, Nakamura Y, Namekawa Y, Taniguchi Y, Ukita N, Yamazaki T and Yoshié T (PACS) 2020 *Phys. Rev. D* **101** 094504 (*Preprint* 1912.13127)
- [20] Moulson M 2017 *PoS CKM2016* 033 (*Preprint* 1704.04104)

¹ <http://luscher.web.cern.ch/luscher/openQCD/>